Hydrostatics and steady dynamics of spatially varying electromechanical flow structures

Thomas B. Jones

Department of Electrical Engineering, Colorado State University, Fort Collins, Colorado 80521
(Received 13 November 1973)

The hydrostatic and steady laminar hydrodynamic equilibria of spatially varying electromechanical flow structures are investigated. Under certain conditions the relationship between the dielectric height of rise and the applied voltage is found to be double valued. It is found that one of the two equilibrium values is always unstable. This gives rise to the experimentally observed spontaneous rise of the fluid to the top of the structure, once a certain critical voltage is reached. Starting above this critical voltage with the structure completely filled and decreasing the applied voltage toward the critical value results in pinch-in failure at an intermediate point along the structure and trapping of dielectric fluid at the top. The simple mathematical model developed predicts all these phenomena, without recourse to tedious point-by-point surface force equilibrium determination. Experiments are reported which verify the results for the hydrostatic case.

I. INTRODUCTION

Using strong nonuniform electric fields provided by properly designed electrodes, poorly conducting dielectric liquids can be oriented and controlled in zero and adverse gravitational environments. This scheme exploits the well-known tendency of dielectrics to be attracted to and collected in regions of higher electric field intensity, with vapor expelled to regions of lower electric field intensity.[1] Proposed applications of this polarization electrohydrodynamical force include the orientation of cryogenic liquids in spacecraft propellant tanks[2] and the electrohydrodynamic heat pipe.[3] A common feature of the two applications cited is the use of polarization forces not merely to collect but also to guide the liquid as it flows. Electrode structures capable of guiding dielectric liquids are examples of electromechanical flow structures, with the liquid partially ducted at "free" surfaces by electrical forces. The dielectric siphon[4] provides an instructive tutorial example of these electromechanical flow structures. The free-surface electrohydrodynamics of these structures are found to be analogous to the surface dynamics of open-channel hydraulics.[5]

While the surface dynamics of electromechanical flow structures are well understood, certain crucial aspects of their hydrostatic and hydrodynamic equilibria are not generally appreciated. These equilibria are important because they determine the conditions under which flow structure failure occurs.

There are two distinct modes of electromechanical flow structure failure. *Excess internal pressure failure* causes an inadvertent expulsion and loss of liquid through the electrically coupled free surfaces. It is apt to occur toward the inlet of the flow structure. This mode does not occur in either of the applications cited above,[2,3] and thus it is not studied here. *Pinch-in failure* causes an inward collapsing of the free liquid surfaces near the outlet end, resulting in loss of axial pressure communication and liquid flow disruption. It occurs when pressure drops due to viscous or gravitational heads become too large. In electrohydrodynamic heat pipe operation,[3] this failure mode has catastrophic consequences. It is therefore essential to develop a theory which predicts the conditions of minimum voltage, maximum flow rate, and maximum adverse gravitational force (tilt) under which an electromechanical flow structure can operate without failure.

II. THEORY

A. Basic electrohydrostatic problem

The simple problem shown in Fig. 1 is easily analyzed theoretically and easily tested experimentally. Moreover, it exhibits the essential features and peculiarities of the hydrostatics and steady dynamics of spatially varying electromechanical flow structures. Two electrode plates are dipped into a large reservoir of an insulating dielectric liquid of permittivity ϵ and mass density ρ_l. The electrode plates are of width w, height H, and small variable spacing $s(z)$. They are stressed by a voltage V. We assume that $s(z) \ll w$ and $s(z) \ll H$. Then the electric field between the plates is essentially horizontal and may be approximated by

$$E(z) \approx V/s(z). \tag{1}$$

Note further that this electric field is primarily tangential to the interface of the elevated liquid between the plates.

1. Dielectric height of rise

The basic calculation of $h(V)$ involves the incompressible hydrostatic equation:

$$\nabla p_l = \overline{F}^e - \rho_l g \hat{z}, \tag{2}$$

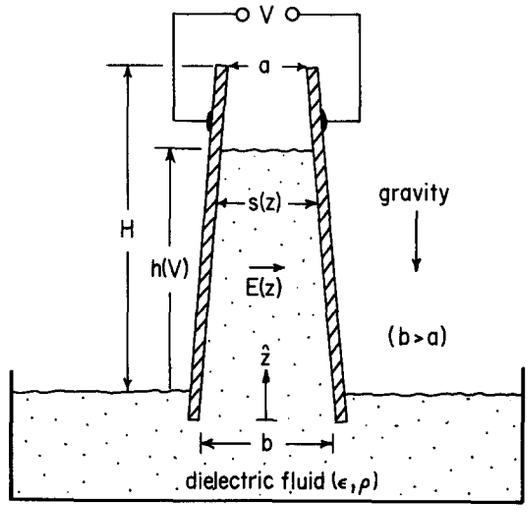

FIG. 1. Spatially varying electrohydrostatic structure.

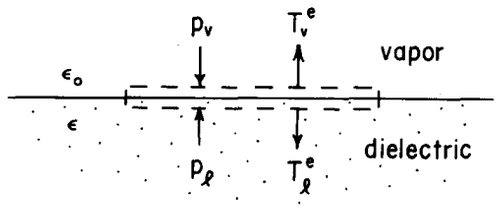

FIG. 2. Dielectric fluid interface for surface force balance.

where

$$\overline{F}^e = -(\tfrac{1}{2}E^2)\nabla\epsilon$$

is the polarization force density,[6] p_l is hydrostatic pressure of the liquid, and g is the gravitational acceleration. Note that in our force density formulation, the dielectric force acts only at electrically stressed interfaces. Integrating Eq. (2) from just under the free surface outside the electrode structure up to just under the electrically stressed interface at $z=h$ yields

$$p_l(z=h) = p_0 - \rho_l g h, \tag{3}$$

where p_0 is the ambient vapor pressure. If we neglect the density of the vapor

$$p_v(z=h) = p_0, \tag{4}$$

where p_v is the pressure of the vapor phase above the liquid interface.

For hydrostatic equilibrium, the sum of all pressure and surface forces at the elevated horizontal interface must be zero (see Fig. 2). For equilibrium

$$p_l - p_v + T_v^e - T_l^e = 0, \tag{5}$$

where surface tension is neglected, and T_v^e and T_l^e are the normal Maxwell stress tensor components just above and below the interface.[7]

$$T_v^e - T_l^e = \tfrac{1}{2}(\epsilon - \epsilon_0)E^2. \tag{6}$$

Combining Eqs. (3)—(6), the result is

$$h = (\epsilon - \epsilon_0)V^2/2\rho_l g s^2(h). \tag{7}$$

If the spacing s is constant, Eq. (7) reduces to the familiar parallel-plate problem.[1]

2. h-V relation

To determine $h(V)$ explicitly, knowledge of $s(z)$ is required. For simplicity, assume a linear relationship,

$$s(z) = b - \alpha z, \tag{8}$$

where $\alpha \equiv (b-a)/H$. Combining Eqs. (7) and (8), a cubic equation in h results. In normalized form, this equation takes the form

$$\underline{h}^3 - 2\underline{h}^2 + \underline{h} - B_e = 0, \tag{9}$$

where $\underline{h} = \alpha h/b$ and $B_e = \alpha(\epsilon - \epsilon_0)V^2/2\rho_l g b^3$ (electrohydrodynamic Bond number). Equation (9) may be solved for $\underline{h}(V)$, and a plot of this dependence is shown in Fig. 3. The relationship is not single valued, leading to speculation as to the voltage-dependent behavior of this hydrostatic equilibrium structure.

3. Important cases

In order to determine the physical significance of the various portions of the $h(V)$ relation plotted in Fig. 3, we must consider the relative magnitudes of H, $h_1 = b/3\alpha$, and $h_2 = b/\alpha$. Three distinct cases must be investigated separately.

Case (i): $H < h_1$. The inequality

$$H < h_1 \tag{10}$$

may be reduced to

$$a < b < \tfrac{3}{2}a \tag{11}$$

For this case, $h(V)$ is a relatively simple monotonic function of the applied voltage.

Case (ii): $h_1 < H < h_2$. The condition

$$h_1 < H < h_2 \tag{12}$$

reduces to

$$b > \tfrac{3}{2}a. \tag{13}$$

For this case, $h(V)$ is double valued in the applied voltage.

Case (iii): $H > h_2$. In this case the inequality

$$H > h_2 \tag{14}$$

reduces to the nonphysical condition $a < 0$, and it may be disregarded. The first two cases (i) and (ii), then, completely describe all physically meaningful situations.

For case (ii), when the inequality (13) holds, $h(V)$ is double valued, indicating that for some range of voltages there are two apparent hydrostatic equilibria. However, it is easily shown that the reverse portion of the curve ($h_1 < h < H$) is unstable. The following physical picture thus emerges for case (ii). When the voltage is increased from zero, the dielectric liquid rises till at a voltage

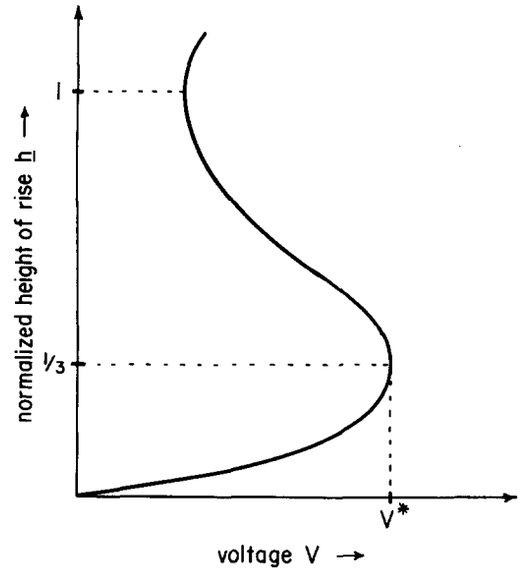

FIG. 3. Theoretical plot of normalized dielectric height of rise $\underline{h}$ vs applied voltage, Eq. (9).

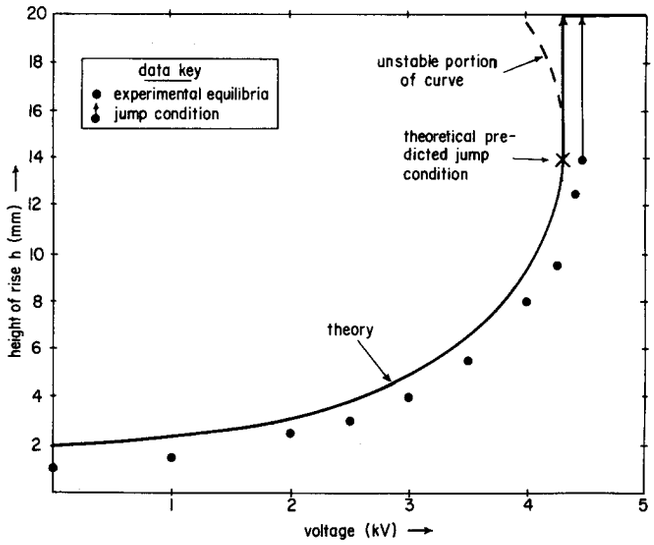

FIG. 4. Plot of theoretical $h(V)$ and experimental data for run No. 5 (fluid: Freon-113®, $b/a = 2.0$, $H = 20$ mm).

$$V^* = [8\rho_1 g b^3/27(\epsilon - \epsilon_0)\alpha]^{1/2}, \tag{15}$$

the liquid has risen to $h = h_1$. Any further increase of the voltage results in a precipitous spontaneous rise of the liquid to the top ($h = H$) (see Fig. 4). On the other hand, if sufficient voltage is applied to fill the entire structure, and then the voltage is decreased to V^* from larger values, it can be shown that pinch-in failure first occurs at $z = h_1$. If the voltage is decreased still further, liquid communication between the upper ($z > h_1$) and lower ($z < h_1$) masses of dielectric liquid is lost and liquid will be trapped at the top of the structure. The behavior of this polarization electrohydrostatic orientation structure is thus hysteretic in nature.

4. Discussion

These results are understood by recognizing that the hydrostatic equilibrium of open "wall-less" structures, such as those shown in Fig. 1, must be defined point by point. There must be sufficient electrical force to maintain hydrostatic pressure differences at the fluid interface for all values of z from zero to h. By generalizing Eq. (5) to apply to all points $0 < z < H$ on the interface, it is easily shown that, if $b > \frac{3}{2}a$, the weakest point in the interfacial hydrostatic equilibrium will be at $z = h_1$. Note that the emergence of this peculiar behavior depends only on the ratio of b to a, and not on α. Similar appealingly simple criteria apply to practical but more difficult to analyze electrohydrodynamic flow structure geometries discussed elsewhere.[5,8]

B. Basic steady dynamic problem

We now add the effect of steady laminar z-directed flow to the problem shown in Fig. 1. We again assume that $\alpha \ll 1$ so that a simple Posiuelle flow model can be used. All the upward flowing liquid is removed at the top liquid surface ($z = h$). Equation (3) of the previous analysis must be modified by a term reflecting the viscous pressure head loss. The new equation is

$$h = \frac{(\epsilon - \epsilon_0)V^2}{2\rho_1 g s^2(h)} - \frac{12\mu \dot{m} h(b - \frac{1}{2}\alpha h)}{\rho_1^2 g w b^2 s^2(h)}, \tag{16}$$

where μ is the dynamic viscosity and $\dot{m}$ is the fluid mass flow rate. Equation (16) reduces to a cubic expression in h and so the new $h(V)$ looks similar to Fig. 3, but the location of the critical point (h_1, V^*) is altered.

$$h_1 = \tfrac{1}{3}b(1 + \gamma), \tag{17}$$

where $\gamma \equiv 12\mu\dot{m}/\rho_1^2 w g b^3$. This problem is analyzed in a fashion similar to the previous hydrostatic example. Several important cases emerge.

Case (1): $\gamma > 2$. For the case

$$\gamma > 2 \tag{18}$$

$h(V)$ is a simple monotonic function of V with no intermediate pinch-in failure points, irrespective of the ratio b/a.

Case 2(a): $0 < \gamma < 2$ and $a < b < 3a/(2 - \gamma)$. For

$0 < \gamma < 2$

and

$$a < b < 3a/(2 - \gamma), \tag{19}$$

the function $h(V)$ is still monotonic.

Case 2(b): $0 < \gamma < 2$ and $b > 3a/(2 - \gamma)$. For

$0 < \gamma < 2$

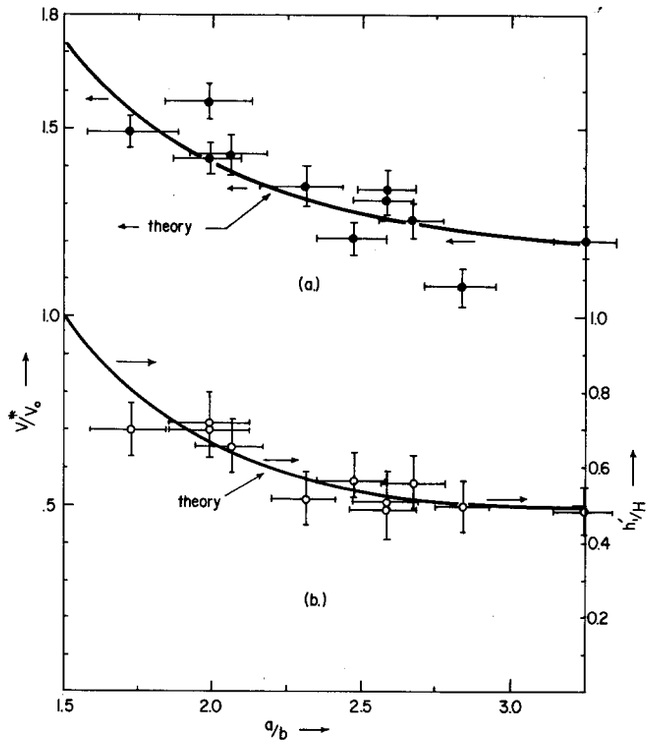

FIG. 5. (a) Theoretical plot of V^*/V_0 vs b/a and experimental data. (b) Theoretical plot of h_1'/H vs b/a and experimental data.

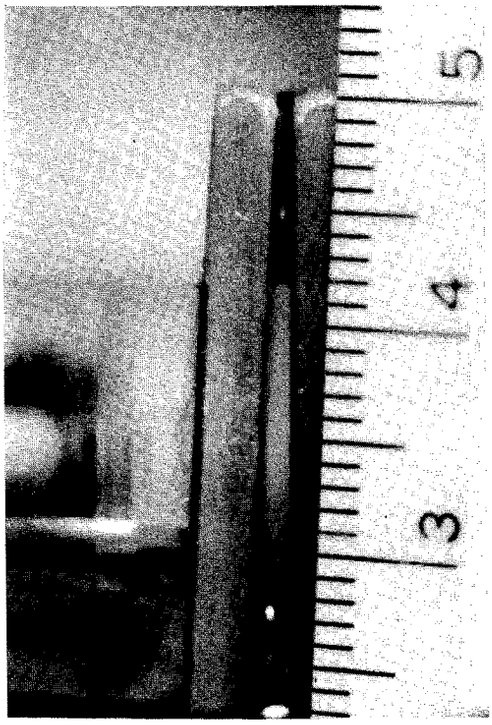

FIG. 6. Photograph showing dielectric fluid trapped at top of spatially varying structure due to intermediate structure failure. (fluid: corn oil).

and

$$b > 3a/(2-\gamma) \tag{20}$$

the function $h(V)$ is doubled valued and behaves much like case (ii) of Sec. IIA 2. The threshold value V^* is increased, as is the value of h_1.

The influence of z-directed mass flow upon the free-surface electrohydrodynamic equilibrium is such as to decrease the likelihood of intermediate pinch-in failure. A flow structure which fails as a result of increasing the flow rate $\dot{m}$ will most likely fail at the highest point rather than at some intermediate position.

For the very special limiting case of $g=0$ and $a=b$, Eq. (16) reduces to the expression derived by Melcher *et al.*[2] for the minimum voltage consistent with laminar hydrodynamic equilibrium.

C. Other dynamic cases

In another dynamic equilibrium problem of interest, it is assumed that the upward flowing liquid is removed along the entire length of the flow structure. This "suction" model is relevant to the electrohydrodynamic heat pipe,[3] because it accurately models the removal of liquid by evaporation from the axial electromechanical flow structure. Still other effects may be important in the determination of the dynamic equilibria of these unique flow structures. Included here are momentum transfer and shear forces exerted by the relatively higher counterflow of vapor in a heat pipe. These and other problems may be modeled by appropriate modifications of Eq. (16).

III. EXPERIMENTS

Experiments with a spatially varying electrohydrostatic structure have been performed as a test on the theory of Sec. II. The experiments reported here are conducted with two different dielectric fluids (Freon-113® and corn oil) and an experimental electrode structure which features adjustable spacing. ac high voltage at frequencies sufficiently high to avoid charge relaxation effects[9] and parametric instabilities[10] is used exclusively (400—600 Hz).

A. Influence of surface tension

The problems of electrical breakdown encountered for normally attainable laboratory conditions requires the use of a small electrode structure (38 mm long with spacing b never exceeding ≈ 2.5 mm). As a result, surface tension effects not included in the hydrostatic model of Sec. IIA become significant, and the theory must be modified to account for their influence. Equation (7) is thus supplemented by a capillary term:

$$h = \frac{(\epsilon-\epsilon_0)V^2}{2\rho_l g s^2(h)} + \frac{2\sigma\cos\phi}{\rho g s(h)}, \tag{21}$$

where σ is the surface tension and ϕ is the wetting angle of the liquid with the electrode plates. Combining Eqs. (8) and (21), one obtains

$$\underline{h}^3 - 2\underline{h}^2 + (1+B_0)\underline{h} - (B_0+B_e) = 0, \tag{22}$$

where $B_0 = 2\alpha\sigma\cos\phi/\rho_l g b^2$ is a conventional (capillary) Bond number. In all the experiments conducted, the condition $B_0 \ll 1$ exists, allowing simple approximate expressions for the threshold voltage V^* and the critical height h_1. To first order in B_0,

$$V^* = [8\rho_l g b^3/27(\epsilon-\epsilon_0)\alpha]^{1/2}(1-\tfrac{9}{4}B_0); \tag{23}$$

$$h_1 = (b/3\alpha)(1+\tfrac{3}{2}B_0). \tag{24}$$

B. Experimental data

Before a typical experimental run, the electrode structure spacings a and b are measured with a thickness gauge. Then, the structure is positioned in the test cell, and the dielectric fluid introduced. The height of rise of the fluid h is measured as the voltage is increased. Also, the voltage at which the fluid jumps up (V^*) and the location of the jump (h_1) are recorded. A typical curve of h versus V is shown in Fig. 4. The correlation of experimental data to theory is within measurement uncertainty. The principal uncertainty is in the measurements of a and b.

A number of experimental runs have been performed at different values of the geometric factor b/a to test the theoretical expressions

$$\frac{V^*}{V_0} = \left(\frac{b/a}{b/a-1}\right)^{1/2}, \tag{25}$$

$$\frac{h_1'}{H} = \frac{b/a}{3(b/a-1)}, \tag{26}$$

where

$$V_0 = [8\rho_l g b^2 H/27(\epsilon-\epsilon_0)]^{1/2}(1-\tfrac{9}{4}B_0),$$

and

$$h_1' = h_1 - \sigma\cos\phi/\rho_l g b.$$

These data are plotted, along with the theoretical curves, in Figs. 5(a) and 5(b). Adequate correlation of theory and experiment is again apparent.

C. Observations of pinch-in failure

Theoretically, it should be possible to obtain experimental values for V^* and h_1 by turning the voltage down from above V^*. It is found, however, that little more than qualitative observation of the pinch-in failure mode is possible, due to surface tension effects. The eventual result of pinch-in failure is depicted in the photograph of Fig. 6, which shows dielectric fluid trapped at the top of the electrode structure. The same failure mode has been observed visually in the electromechanical flow structure of an electrohydrodynamic heat pipe experiment.[8]

IV. DISCUSSION

The expanded class of electrohydrostatic and electrohydrodynamic structures considered here has been found to exhibit interesting behavior which may be analyzed using a very simple model. Proper interpretation of the results of analysis allows prediction of intermediate pinch-in failure for various flow structures, without recourse to a point-by-point equilibrium determination. The intermediate pinch-in failure phenomenon is found to occur only in structures with spatially varying character of easily defined form. For the linearly varying case considered (see Fig. 1), the observation of intermediate failure is confined to structures with sufficiently large b/a. The presence of fluid motion does modify the fundamental criterion for intermediate failure, viz., Eq. (13).

These results may be applicable to a variety of electromechanical flow structures discussed in the literature,[2-5,8] Because of the considerable analogy of the behavior of ferrofluids[11] in magnetic fields, similar ferrohydrostatic and dynamic effects are anticipated. Using the electrode structure of Fig. 1 as a building block, a new electrohydrodynamic pumping scheme for dielectrics may be envisioned.

ACKNOWLEDGMENT

This work was supported in part by the National Aeronautics and Space Administration, Ames Research Center.

[1]H. Pellat, C.R. Acad. Sci. (Paris) **119**, 675 (1894).
[2]J.R. Melcher, M. Hurwitz, and R.G. Fax, J. Spacecr. Rockets **6**, 961 (1969).
[3]T. B. Jones, Int. J. Heat Mass Transfer **16**, 1045 (1973).
[4]T. B. Jones, M.P. Perry, and J.R. Melcher, Science **174**, 1232 (1971).
[5]T. B. Jones and J.R. Melcher, Phys. Fluids **16**, 393 (1973).
[6]J.A. Stratton, *Electromagnetic Theory* (McGraw-Hill, New York, 1941), p. 139.
[7]H.H. Woodson and J.R. Melcher, *Electromechanical Dynamics* (Wiley, New York, 1968), Part 2, Chap. 8.
[8]T. B. Jones and M.P. Perry, Report No. NASA CR-114498, 1972 (unpublished).
[9]J.R. Melcher and W.J. Schwartz, Phys. Fluids **11**, 2604 (1968).
[10]T. B. Jones, J. Appl. Phys. **43**, 4400 (1972).
[11]J.L. Neuringer and R.E. Rosensweig, Phys. Fluids **7**, 1927 (1964).